Journal of Energy

ISSN 1849–0751 (On–line)
ISSN 0013–7448 (Print)
UDK 621.31

https://doi.org/10.37798/EN2022712

VOLUME 71 Number 2 | 2022

71

ENERGIJA

Journal of Energy

Scientific Professional Journal Of Energy, Electricity, Power Systems
Online ISSN 1849–0751, Print ISSN 0013–7448, VOL 71
https://doi.org/10.37798/EN2022712

Published by
HEP d.d., Ulica grada Vukovara 37, HR–10000 Zagreb
HRO CIGRÉ, Berislavićeva 6, HR–10000 Zagreb

EDITORIAL

Igor Kuzle
Editor–in–Chief

Journal of Energy

VOLUME 71 Number 2 | 2022

journal homepage: http://journalofenergy.com/

Development of a Battery Management System for Centralized Control of a Battery Cluster

Tamara Trogrlić, Mateo Beus

***Summary* — The purpose of this paper is to establish a supervisory battery management system which collects active power, reactive power and state of charge measurements from the installed battery storage units and enables active and reactive power control. In addition, an HMI user interface was designed to allow the user to monitor and control the batteries. The batteries communicate with the PLC via Modbus TCP/IP protocol. The communication enables the exchange of measured power and state of charge values between the PLC and batteries, as well as setting the desired power setpoint values and battery activation signals. The PLC and HMI communicate via PROFINET. The battery storage units are installed in Smart Grid Laboratory (SGLab) at the University of Zagreb Faculty of Electrical Engineering and Computing.**

***Keywords* — battery management system, Modbus TCP/IP, PLC, HMI, user interface.**

I. Introduction

At a time when the impact of electric power industry on the environment is gaining importance, new technologies are being developed to help the power system face the challenges of integrating renewable power sources into the system. An example of these new technologies which can help increase the flexibility of the existing power system are batteries, especially when used with photovoltaic (PV) systems. In that regard, the authors in [1] introduced the control strategy to achieve decentralized power management of a PV/battery hybrid unit in a droop-controlled islanded microgrid. Furthermore, the authors in [2] introduced a control strategy designed for hybrid energy storage system. In the proposed control strategy battery storage is used to compensate for slow charging power surges, while supercapacitors are applied to compensate for the fast charging surges. Additionally, in [3] the authors analyzed the configuration, design and operation of a grid with large PV penetration. In order to increase operational flexibility the proposed grid configuration also included a utility scale battery storage system connected to the grid through an independent inverter. In [4], a hybrid control strategy for PV and battery storage system in a stand-alone DC microgrid is proposed. Researchers in [5] developed a control strategy to achieve fully autonomous power management of multiple photovoltaic (PV)/battery hybrid units in islanded microgrids. The control strategy introduced in that paper had the ability to autonomously coordinate with dispatchable droop controlled units. By and large, batteries require a monitoring and control system to maximize their efficiency, but also to help re- searchers to better understand and improve existing technolo- gies. Interesting research in terms of the BMS development has been presented in [6]- [8]. In that regard the authors in [6] presented the BMS design for the application in the electric vehicles, while the authors in [7] introduced an advanced BMS for the application in smart grid infrastructure. In [8] the authors developed a hardware-in-the-loop (HIL) simulation battery model for purposes of BMS testing on a commercial HIL simulator. Additionally, in [9]- [10] the authors provided an extensive overview of the BMS designs for the application in the smart grid environment. Furthermore, the papers [11]- [12] deal with the advanced design of the BMS. In [11] the authors presented design and implementation of a BMS for the industrial internet of things (IIoT) enabled applications, while in [12] the authors presented the development of a BMS whose operation is based on the application of an Multi-Objective Gravitational Search Algorithm to schedule the best battery allocation.

Furthermore, the authors in [13] elaborated the concept of a virtual inertia provision using battery energy storage system.

This paper describes the development of a supervisory BMS (Battery Management System) application for battery units applied in households. The control algorithm is implemented using a PLC (Programmable Logic Controller), while the HMI's (Human-Machine-Interface) touch panel enables an intuitive user-friendly interface. The main goals of the designed BMS were to collect the chosen measurements from the batteries and display them on the HMI screen, and to create both active and reactive power management functions as well as SOC balancing functions. Establishing the communication between the batteries, PLC and HMI was of the utmost importance for the BMS to work. The paper is structured as follows. The established laboratory setup that is used for development of the BMS is described in the Section II. Section III provides a detailed overview of the developed BMS, from establishing communication to the designed functionalities. Experimental results are presented in the Section IV.

II. Laboratory Setup

This section gives an overview of VARTA Pulse 6 energy storage [15], SIMATIC ET200-SP PLC [18] and SIMATIC

TP1200 Comfort Panel HMI device [20]. Figure 1 illustrates the general overview of the equipment that is used to establish

(Corresponding author: Mateo Beus)

Tamara Trogrlić and Mateo Beus are with the University of Zagreb Faculty of Electrical Engineering and Computing,

Zagreb, Croatia (e-mail: tamara.trogrlic@fer.hr, mateo.beus@fer.hr)

Tamara Trogrlić, Mateo Beus, Development of a Battery Management System for Centralized Control of a Battery Cluster, Journal of Energy, vol. 71 Number 2 (2022), 3–9

https://doi.org/10.37798/2022712415

the necessary laboratory setup. As shown in Figure 1 the-communication network used to establish the laboratory setup is Ethernet-based and uses Modbus TCP and PROFINET industrial communication protocols.

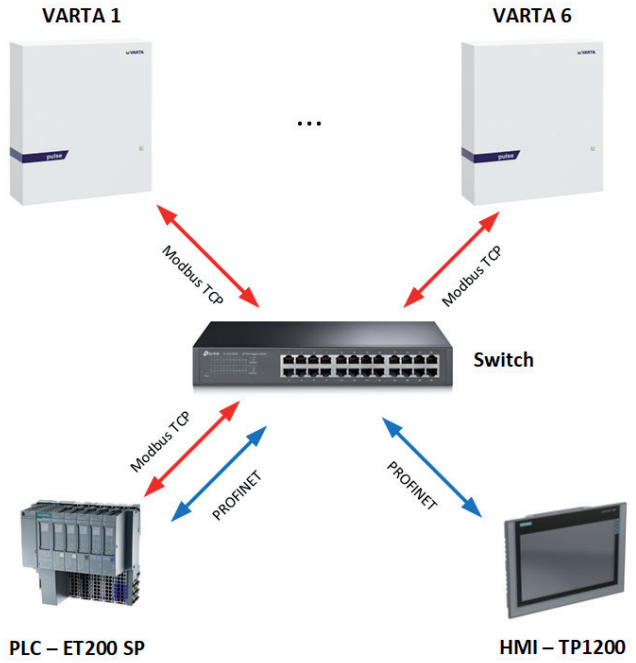

Fig. 1. General overview of the laboratory setup in SGLab

hand, if the PV energy production does not meet the object's needs, the electric current direction is from the grid into the object and the battery is discharged (if it has a sufficient SOC) with the goal to minimize the consumption of electrical energy from the grid. However, it is important to note that the above-mentioned sensor is disabled in the current laboratory setup so that the battery storage units can be controlled from an external system, such as a SCADA (Supervisory Control and Data Acquisition) system. Each battery storage unit is equipped with an Ethernet interface that was used to establish communication with the PLC via the Modbus TCP/IP protocol. Figure 2 shows the installed battery units in the lab.

Fig. 2. VARTA Pulse 6 battery units in SGLab

A. VARTA Pulse 6 energy storage

To explore the possibilities of energy storage systems and the-ir monitoring and management capabilities, six VARTA Pulse 6 battery storage units were installed in the Smart Grid Laboratory (SGLab) at the University of Zagreb Faculty of Electrical Engineering and Computing [14]. Since each battery unit has a single-phase inverter, a pair of two battery units is connected in each phase in order to establish a well balanced three-phase battery storage system.

The batteries' technical characteristics are displayed in Table I.

TABLE I

VARTA Pulse 6 technical characteristics [14]

Nominal capacity	6.5 kWh
Max. AC charge/discharge power	2.5/2.3 kW
Depth of discharge	90%
Electrochemistry	NMC
Mains connection	230V AC, 50 Hz, 1-phase
Mains configuration	TT-systems, TN-systems
Max. current output	11A
Protection class	IP33
Ambient conditions	+5°C to +30°C
Recommended circuit protection	B 16A MCB

First and foremost, the described battery storage system is designed for use in households with installed PV systems to get the most out of the locally produced energy [16]. With that in mind, an electric current sensor which controls the charging and discharging is included in the battery storage system's additional equipment. The sensor is installed just after the electricity meter and monitors the electric current direction: if the direction is from the object into the grid while the battery's state of charge (SOC) is less than the maximum SOC, the battery is charged. On the other

B. Programmable Logic Controller SIMATIC ET200-SP

SIMATIC ET200-SP station is a flexible, modular, and compact system from Siemens for various automation ap- plications. The station configuration can expand up to 64 modules, including digital and analog I/O modules [17]. I/O modules were not used for this application, since all necessary inputs and outputs are exchanged via Modbus TCP between the PLC and batteries. Using an interface module enables the communication with a central PLC if the station is used as distributed I/O [18]. The PLC has a CPU 1512SP-1 PN module with the functionalities of a Siemens S7-1500 series CPU [19]. The module has a 3-port PROFINET interface. Ports 1 and 2 require a bus adapter, while port 3 has an integrated RJ45 socket. The CPU module needs a 24V DC power supply and has a reverse polarity protection. A server module, which serves as an electrical and mechanical con- nection to the backplane bus and enables the monitoring of power supply voltage, is added to the CPU module. The CPU allows for up to 4000 defined blocks, which include Data Blocks (DB), Function Blocks (FB), Functions (FC), and Organizational Blocks (OB). The developed BMS algo- rithm uses two Organisational Blocks (OBs). The first OB1

- Main (contains Functions (FCs) which output final active and reactive power setpoints and activation signals) and OB30

- Communication (contains configured Modbus Clients and power monitoring functions). The block Main is executed with each PLC cycle, while Communication is a cyclic interrupt block which executes every 100 ms. Cyclic interrupt is used since the measured values don't change rapidly and such a delay in sending setpoint values to the batteries is insignificant. The FC's in Main use auxiliary FC's responsible for smaller tasks, such as a FC used for SOC regulation which checks the SOC of a battery and determines the corresponding power setpoint. Data Blocks (DBs) are

Tamara Trogrlić, Mateo Beus, Development of a Battery Management System for Centralized Control of a Battery Cluster, Journal of Energy, vol. 71 Number 2 (2022), 3–9
https://doi.org/10.37798/2022712415

used to organize measured and calculated data, as well as parameters needed for Modbus clients. The PLC supports following programming languages (IEC 61131-3): LAD (Ladder Diagram), FBD (Function Block Diagram), STL (Statement List), SCL (Structured Control Language) and GRAPH. LAD programming language was used for programming the BMS application in the PLC. The CPU supports various communications protocols, such as IP protocol, PROFINET IO, Open IE communication, OPC UA and Modbus TCP. It can have up to 128 simultaneously active connections, including those connected either via the CPU's integrated interfaces or via the communication processor mod- ule. Furthermore, the PLC can be connected to the Human – Machine Interface (HMI) via PROFINET to allow the user to easily control and monitor the battery storage units by means of a graphic user interface, which will be discussed later. The connection is created in the *Devices and networks* window of TIA Portal by connecting the Ethernet ports of the PLC and the HMI. The PLC and HMI are then in the same subnet. Their IP addresses must be set accordingly. In addition to having unique IP addresses, the devices communicating via PROFINET also need to have unique PROFINET device names.

C. SIMATIC TP1200 Comfort Panel

The chosen HMI device for this application is a SIMATIC TP1200 Comfort Panel from Siemens, which is designed as a touch screen. It has a TFT (thin-film-transistor) display, which is an LCD (liquid-crystal display) variant, with a 12.1-inch screen diagonal [20]. Control elements include only numeric and alphanumeric onscreen keyboards, but can be expanded with up to 40 direct keys (touch buttons). The required supply voltage is 24V DC, with a permissible range between 19.2V and 28.8 V. The panel has an x86 type processor, Flash and RAM memory, and 12 MB available memory for user data. It comes with a pre-installed Windows CE operating system. The panel is equipped with a 2-port industrial Ethernet interface, one RS-485 interface and two USB 2.0 interfaces. The supported protocols include PROFINET, PROFIBUS, EtherNet/IP, MPI, IRT and PROFINET IO. HMI can be configured from TIA Portal, using either a WinCC Comfort, WinCC Advanced or WinCC Professional software. There is a message system with 32 alarm classes and configurable acknowledgement groups. In addition, recipe management is a particularly interesting functionality for industrial automation. The HMI can be used for process monitoring and control in combination with PLCs from manufacturers other than Siemens, such as Allen Bradley and Mitsubishi. Laboratory setup used for testing is shown in Figure 3. It consists (from left to right) of a 24V DC industrial power supply, the PLC, a network switch, the HMI and a laptop. The power supply powers the PLC and HMI. The PLC, HMI, batteries and laptop are connected to the switch using Ethernet cables so that they are in the same LAN network. The HMI's main screen (with default values, before reading the battery measurements) is displayed in Figure 4. It shows the batteries as icons and displays the measured active, reactive and apparent power values, as well as the SOC for each battery. Total active, reactive and apparent power values can be seen at the bottom of the screen. A drop-down menu for choosing the screen for different control mode (active/reactive power control and SOC control) can be seen in the bottom right corner.

There are separate screens for active power/SOC regulation and reactive power regulation, but their working principle is the same. First and foremost, a management function variant must be selected on the screen. Once it is selected, the corresponding input fields and switches appear on the screen. The screen allows manipulating the inputs of the selected func- tion only. If the selected active power management function changes, all battery units are deselected to prevent them from accidentally following another management function's outputs. However, if the selected reactive power regulation function changes, all reactive power setpoints are just reset to zero, to avoid affecting the battery unit selection of active power management functions.

To finish connecting the HMI with the PLC, a connection has to be created in HMI's *Connections* tab in the TIA Portal. The connection parameters include the interface type and the devices' IP addresses. The created connection is later used to link the HMI tags with the corresponding PLC tags. Objects, such as I/O fields, buttons and text fields, are added to the screens using drag-and-drop and linked to HMI tags. Layers were used to reduce the number of screens. Screen objects that belong to the same function were arranged in the same layer and their visibility was set so that they are visible only when that function is selected. The HMI collects user-controlled inputs which get forwarded to the PLC. The PLC performs the programmed logic using these inputs and sends the necessary outputs to the HMI so the process can be monitored by the user.

D. Modbus TCP/IP communications protocol

Modbus is a communications protocol developed in 1979 by the Modicon company. It is widely used in industrial automation thanks to its simplicity and flexibility. Master/slave is main working principle of the Modbus RTU or client/server in case of Modbus TCP. Slave devices receive data from or send data to a master device only upon getting a request from a master device. Slave devices cannot volunteer data. Every device communicating via Modbus is required to have

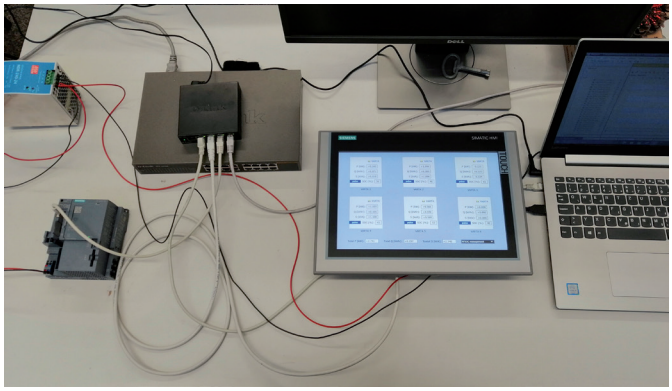

Fig. 3. Laboratory setup for BMS testing

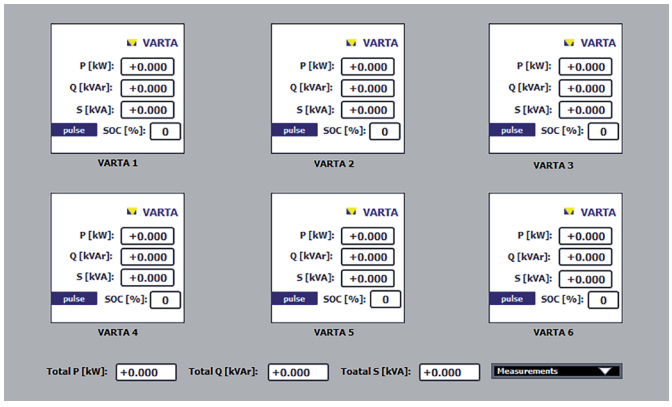

Figure 4. HMI main screen of developed BMS

a unique address. The most common variations of the Modbus protocol are Modbus RTU, Modbus ASCII, and Modbus TCP. Modbus RTU and Modbus ASCII are serial protocols which use a RS-232 or RS-485 interface, while Modbus TCP follows the OSI network model and can be used over the Ethernet infrastructure.

Another difference is that when using Modbus RTU and Modbus ASCII, there can be only one master device in the network, while Modbus TCP allows for multiple servers accessed by multiple clients. To use Modbus TCP, IP addresses of all devices in the network must be known. Modbus client device sends data to port 502 on server devices. Server device register types are listed in Table II [21].

TABLE II

MODBUS REGISTER TYPES

Memory block	Data type	*Client* access	*Server* access
Coils	Bool	read/write	read/write
Discrete inputs	Bool	read-only	read/write
Holding registers	Word	read/write	read/write
Input registers	Word	read-only	read/write

Address spaces for the above-mentioned memory blocks are: 00001-09999 for coils, 10001-19999 for discrete inputs, 20001-29999 for holding registers and 30001-39999 for input registers. The first digit of the address area determines the type of the register, and the remaining digits its location. Every Modbus command contains the address of a slave device that needs to be accessed, and a checksum to detect transmission errors. Modbus register table must be given for a device to know the addresses of its registers and what they stand for. In addition to the above, Modbus commands also contain Modbus function codes which define the desired action for the addressed register. Modbus functions can be regarded as either read or write functions and can moreover be differentiated by the type of the register being accessed. For example, the function code 3 stands for reading multiple holding registers. Exception codes are defined to help find the problem in case of a failed communication.

III. THE DEVELOPED BMS APPLICATION

A. ESTABLISHING COMMUNICATION OF THE PLC WITH THE BATTERIES

Successfully establishing the communication of the PLC with the batteries and the HMI is the first step to creating a battery management system. The PLC communicates with the battery storage units via Modbus TCP protocol over an Ethernet network. It enables retrieving the following mea- surements from the batteries: active power, apparent power, and state of charge. Furthermore, it enables sending the active and reactive power setpoints, along with an on/off signal, to the batteries. The absolute value of reactive power for each unit is calculated from the active and apparent power because the dedicated Modbus register for its measurement does not exist in the battery storage units. PLC acts as a Modbus client device, while the batteries have the role of a Modbus server. To establish a connection between the PLC and a battery storage unit, an already existing system function block in TIA Portal, called MB CLIENT, was used. One MB CLIENT represents one connection, and every connection needs a separate ID. Ev- ery battery needs separate connections for read and write func- tions because Modbus mode (MB MODE), which includes the Modbus function code, is an input to the MB CLIENT function block. Input parameters also include data address and data length, which together determine how many registers to read, starting at the given address, set according to the Modbus register table of the batteries. MB CLIENT needs a memory location for saving the acquired data or from which to send the data to the battery. Request and Disconnect parameters define if the communication requests are being sent and if the connection with the device is established, respectively. The last important input parameter is Connect, which contains the PLC's hardware-defined Ethernet interface ID, the connection ID, connection type, the requested device's IP address and the port number on the battery unit [22]. A separate data block was created for each connection, and it contains the described parameter configuration for the respective connection, along with an array in which the read data is stored or from which the data is written to the battery. An example of a data block with the above-mentioned parameters is given in Figure 5. That data block configures the connection for reading the data from the first battery. In total, 18 connections were created, 6 of which are used for reading the measurements, and the rest are used for writing power setpoints and on/off signals (since the reactive power setpoint register is not positioned

MB_Client_1R

	Name	Data type	Start ...	Comment
1	Static			
2	REQ	Bool	true	
3	DISCONNECT	Bool	false	
4	MB_MODE	USInt	103	Read multiple holding registers.
5	MB_DATA_ADDR	UDInt	1066	Start address.
6	MB_DATA_LEN	UInt	3	Number of registers.
7	Data_Varta1_R	Array[1..3] of Int		
8	Data_Varta1_R[1]	Int	0	Active power [W]
9	Data_Varta1_R[2]	Int	0	Apparent power [W]
10	Data_Varta1_R[3]	Int	0	SOC
11	STATUS	Word	16#0	
12	CONNECT	TCON_IP_v4		
13	InterfaceId	HW_ANY	64	HW-identifier of IE-interface submodule
14	ID	CONN_OUC	1	connection reference / identifier
15	ConnectionType	Byte	11	type of connection: 11=TCP/IP, 19=UDP (17
16	ActiveEstablished	Bool	true	active/passive connection establishment
17	RemoteAddress	IP_V4		remote IP address (IPv4)
18	ADDR	Array[1..4] of Byte		IPv4 address
19	ADDR[1]	Byte	192	IPv4 address
20	ADDR[2]	Byte	168	IPv4 address
21	ADDR[3]	Byte	66	IPv4 address
22	ADDR[4]	Byte	75	IPv4 address
23	RemotePort	UInt	502	remote UDP/TCP port number
24	LocalPort	UInt	0	local UDP/TCP port number

Fig. 5. MB CLIENT configuration parameters

immediately after target power and on/off signal registers, it cannot be simply written using the same MB CLIENT). Finally, all MB CLIENT blocks are gathered in a dedicated function in the cyclic interrupt block OB35, which is executed every 100 milliseconds.

B. BATTERY MANAGEMENT FUNCTIONS

The main purpose of this paper was to create the BMS and its corresponding HMI application. On the HMI's main screen, the battery storage units are represented as icons showing their respective active power, reactive power, apparent power, and state of charge measurements. The main screen also includes the batteries' combined active power, reactive power, and apparent power measurements.

1) Measurement acquisition and display: Measurements are acquired every time the OB35 cyclic interrupt block executes and are saved in their predefined memory locations. Since the power is measured in watts, but has to be displayed in kilowatts, an additional function was created to modify the acquired measurements. The function also calculates the batteries' reactive power, as seen in Equation 1, where Q_i is the i-th battery's reactive power in kilowatts while S_i and P_i are the i-th battery's apparent and active power in watts, respectively.

$$Q_i = \frac{\sqrt{S_i^2 - P_i^2}}{1000} \qquad i = 1, .., 6 \qquad (1)$$

Tamara Trogrlić, Mateo Beus, Development of a Battery Management System for Centralized Control of a Battery Cluster, Journal of Energy, vol. 71 Number 2 (2022), 3–9
https://doi.org/10.37798/2022712415

Reactive power sign is afterwards determined from the sign of the input percentage in reactive power regulation function. In addition, the same function is used to calculate the combined active power, reactive power, and apparent power values for display on the HMI's main screen. There is one HMI screen dedicated to the trend view of measured values and some setpoint values. It allows the user to select whether he wants to see active power, reactive power or SOC values by pressing the onscreen buttons. It also shows the user which management functions are selected, so the user knows which values to focus on.

2) Management functions: The BMS consists of three main management functions: active power regulation, which has two variants, SOC regulation with two variants and reactive power regulation, which also has two variants. Functions have their dedicated screens, where the user can select the management function variant and input the desired setpoints though the HMI's touch screen. Moreover, active and reactive power regulation should theoretically be able to operate indepen- dently, but it was found during laboratory testing that for reactive power regulation to work properly, the selected battery unit's active power setpoint must be different than zero (in other words, the batteries cannot have a solely reactive power output).

3) Active power regulation: Active power regulation has the following variants:

- Unit active power regulation: each battery unit's active power setpoint is set separately
- Group active power regulation: one active power setpoint is divided amongst the battery units

There is a dedicated function in the PLC which gathers all the necessary inputs for all variants, but only executes the code designed for the selected variant. The outputs of the function are final active power setpoints (integer value, in watts, as is required by the battery units) that are sent to the batteries via Modbus TCP, using the configured Modbus clients. The batteries have internal regulators which correct the setpoints if they are out of the allowed range.

Unit active power regulation allows the user to set a different charging (positive value) or discharging (negative value) power setpoint for each battery, as well as to turn the battery on or off. Active power setpoints are set through the HMI's input fields, while the on/off functionality is implemented as a switch. Input fields and switches (for all described functions) are connected to the HMI's corresponding tags, which are in turn connected to the PLC tags. These tags are inputs to the dedicated function in the PLC. That function takes care of making the necessary adjustments to the inputs, such as converting the data type and unit of measurement (kilowatts to watts). The HMI screen which enables the described unit active power regulation is shown in Figure 6.

Group active power regulation enables the user to input a sin- gle active power setpoint (either a positive or a negative value), which then gets equally divided amongst the six batteries. All battery units are activated or deactivated simultaneously using one switch on the HMI screen. The PLC function calculates the setpoint which gets sent to the batteries and once again makes the necessary adjustments.

4) SOC regulation: State of charge regulation is designed as follows:

- Unit SOC regulation: each battery unit's state of charge setpoint is set separately
- Group SOC regulation: all battery units get the same state of charge setpoint

SOC regulation is handled by the same function as active power regulation since it ultimately modifies active power

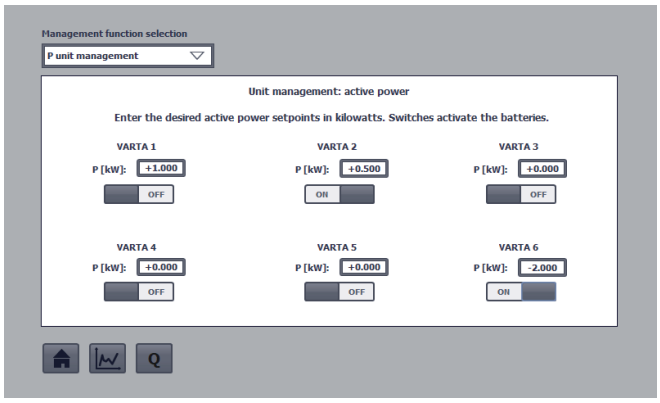

Fig. 6. Unit active power regulation HMI screen

setpoints.

Unit SOC regulation is focused on separately setting the desired state of charge setpoints (from 0% to 100%) for the batteries. The batteries are selected (but not activated or deactivated) via the already described switches. The algorithm is as follows: the function subtracts the selected battery's measured SOC from the SOC setpoint and takes the absolute value of the result. Active power setpoint magnitude is picked from four predefined values, shown in Table III, based on the calculated result (if the result is not zero). Greater SOC

TABLE III

CHARGING/DISCHARGING POWER VALUES DEPENDING ON THE SOC DIFFERENCE

/ΔSOC/ [%]	Charging/discharging power [W]
[50, 100]	2000
[30, 50)	1500
[10, 30)	1000
[0, 10)	500

difference results in a greater active power setpoint magnitude. If the measured SOC is greater than the SOC setpoint, the active power setpoint is sent to the function output as a negative value (discharging). If the measured SOC is lower than the SOC setpoint, the active power setpoint is sent to the function output as a positive value (charging). After the power setpoint is determined, the function output for battery activation is set accordingly. The outputs are sent to the battery units. This algorithm is repeated, adjusting the power setpoint as the battery charges or discharges, until the measured SOC matches the SOC setpoint or until the battery gets deselected. Then the power setpoint is 0, and the battery is deactivated. Group SOC regulation is very similar to Unit SOC regulation, the difference being that the same SOC setpoint is given for all batteries and all batteries are selected simultaneously. Determining the individual battery's active power setpoint and activation signal follows the same logic as described above.

5) Reactive power regulation: Reactive power regulation has the following variants:

- Unit reactive power regulation: each battery unit's reac- tive power setpoint is set separately
- Group reactive power regulation: one reactive power setpoint is divided amongst the battery units

As stated before, reactive power regulation requires the target

Tamara Trogrlić, Mateo Beus, Development of a Battery Management System for Centralized Control of a Battery Cluster, Journal of Energy, vol. 71 Number 2 (2022), 3–9
https://doi.org/10.37798/2022712415

battery storage unit to have an active power setpoint different than zero. There is a dedicated PLC function, which collects necessary inputs for both variants, but executes only the code needed for the selected variant. The function outputs are reactive power setpoints that are sent to the batteries via Modbus TCP.

Unit reactive power regulation enables the user to set a different reactive power setpoint for each battery. As opposed to the active power setpoints, reactive power setpoints must be set as a percentage of the rated power value, in a range [- 100%, 100%] for capacitive and inductive power, respectively. After ensuring that the input value is within limits, it gets forwarded to the output. Conversion of the set percentage into actual reactive power value is handled by the internal battery regulator and as such cannot be manipulated any further.

Group reactive power regulation allows the user to input a desired reactive power percentage setpoint, which then gets equally divided amongst the six battery units. The described functionality is shown by a flowchart in Figure 7. It must be noted that the sign of the input percentage is used to determine the sign of the reactive power value displayed on the main screen icons, since the batteries' displayed reactive power is not measured, but calculated from the apparent and active power values. Reactive power regulation is important because

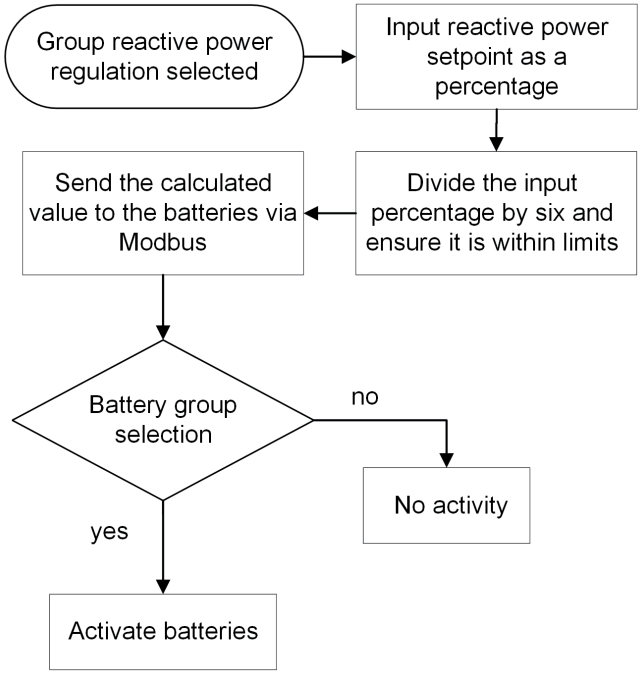

Fig. 7. Group SOC regulation flowchart

it enables voltage regulation using the battery units. Further insight into that functionality is beyond the scope of this paper.

6) Activating and deactivating the battery storage units: Since all management functions manipulate the activation and deactivation of batteries, an additional function was created to take all those influences into account. The function in- puts include the management function selection, HMI screen switches, and the on/off outputs of Unit SOC regulation and Group SOC regulation functions. The function contains a logic designed to determine whether a battery should be activated or not. The function's outputs are on/off signals for the batteries and are written to the batteries' respective registers via Modbus TCP.

IV. Experimental Results

The application was tested in SGLab using the described setup. The responses of the battery units to Group active power regulation and Group SOC regulation were recorded using TIA Portal's Trace functionality. Responses were plotted using Matlab. Figures 8 and 9 show the responses.

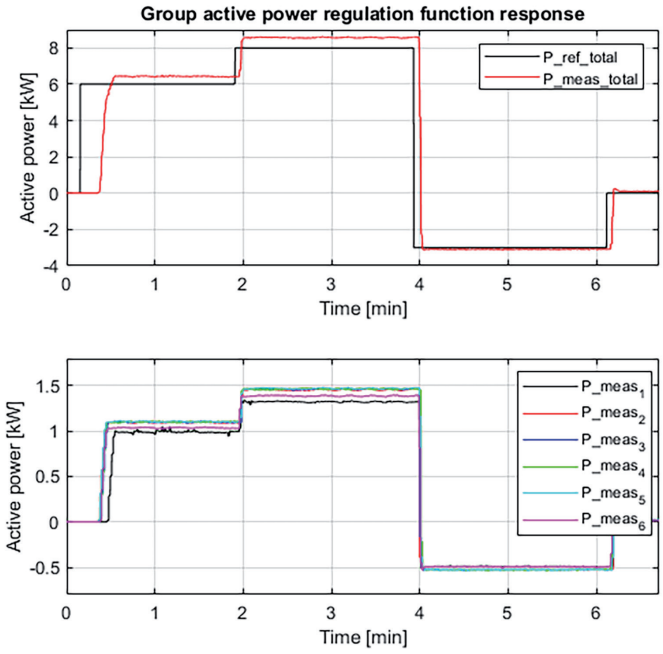

Fig. 8. Group active power regulation function response

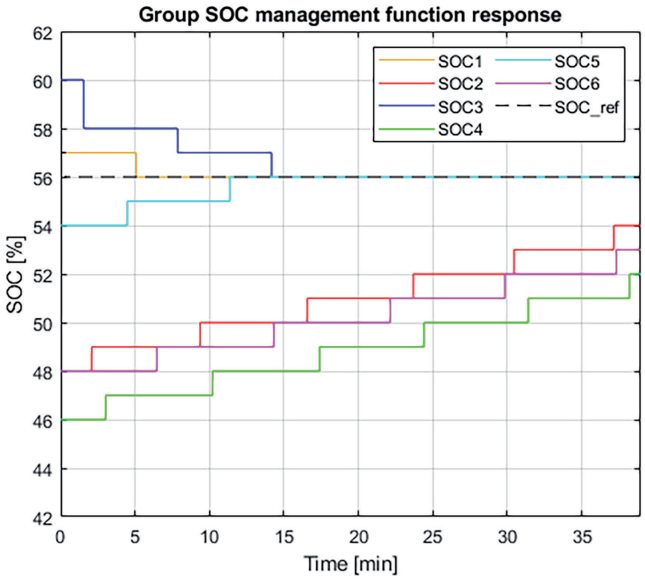

Fig. 9. Group SOC management function response

The first subplot in Figure 8 shows how the measured total active power follows the combined active power setpoint. The measured value varies slightly from the setpoint value because the internal controllers of the battery units can not precisely follow the setpoint value. The second subplot shows the distribution of the total measured active power amongst the batteries.

Figure 9 shows each battery's response to the Group SOC management function. The SOC setpoint is set to 56% for all batteries. Each battery initially had a different SOC value. It can be seen from the plot that the battery units 1, 3 and 5 reached

Tamara Trogrlić, Mateo Beus, Development of a Battery Management System for Centralized Control of a Battery Cluster, Journal of Energy, vol. 71 Number 2 (2022), 3–9
https://doi.org/10.37798/2022712415

the desired setpoint during the recorded interval, while the battery units 2, 4 and 6 are approaching the setpoint value.

V. Conclusion

This paper presents a battery management system developed for the six VARTA Pulse 6 battery storage units located in SGLab at the University of Zagreb Faculty of Electrical Engineering and Computing. The BMS was developed as a PLC application and enables monitoring and control of the installed batteries. Furthermore, an HMI user interface was created for the BMS. The user interface displays measurements obtained from the batteries and allows the control of the battery units through the HMI's touch panel. The introduced laboratory setup meets the set goals and can serve as a basis for the development of the voltage control algorithms or energy management systems that can be applied in low-voltage microgrids.

References

[1] H. Mahmood, D. Michaelson and J. Jiang, "Decentralized Power Man- agement of a PV/Battery Hybrid Unit in a Droop-Controlled Islanded Microgrid," *IEEE Trans. on Power Elec.*, vol. 30, no. 12, pp. 7215–7229, 2015.

[2] S.K. Kollimalla, M.K. Mishra and N.L. Narasamma, "Design and Analysis of Novel Control Strategy for Battery and Supercapacitor Storage System," *IEEE Trans. on Sust. Energy*, vol. 5, no. 4, pp. 1137– 1144, 2014.

[3] V. Rallabandi, O.M. Akeyo, N. Jewell and D.M. Ionel, "Incorporating Battery Energy Storage Systems Into Multi-MW Grid Connected PV Systems," *IEEE Trans. on Ind. App.*, vol. 55, no. 1, pp. 638–647, 2019.

[4] H.W. Yan et. al., "Minimizing Energy Storage Utilization in a Stand- Alone DC Microgrid Using Photovoltaic Flexible Power Control," *IEEE Trans. on Smart Grid*, vol. 12, no. 5, pp. 3755–3764, 2021.

[5] H. Mahmood and J. Jiang "Autonomous Coordination of Multiple PV/ Battery Hybrid Units in Islanded Microgrids," *IEEE Trans. on Smart Grid*, vol. 9, no. 6, pp. 6359–6368, 2016.

[6] K.W.E. Cheng, B.P. Divakar, H. Wu, K. Ding and H.F. Ho "Battery- Management System (BMS) and SOC Development for Electrical Vehi- cles," *IEEE Trans. on Vehicular Technology*, vol. 60, no. 1, pp. 76–88, 2011.

[7] A.T. Elsayed, C.R. Lashway and O.A. Mohammed "Advanced Battery Management and Diagnostic System for Smart Grid Infrastrucutre," *IEEE Trans. on Smart Grid*, vol. 7, no. 2, pp. 897–905, 2016.

[8] J.V. Barreras et al. "An advanced HIL Siumlation Battery Model for Battery Management System testing," *IEEE Trans. on Industry Appli- cations*, vol. 52, no. 6, pp. 5086–5099, 2016.

[9] H. Rahimi-Eichi, U. Ojha, F. Baronti and Mo-Yuen Chow "Battery Management System: An Overview of Its Application in the Smart Grid and Electric Vehicles," *IEEE Industrial Electronics Magazine*, vol. 7, no. 2, pp. 4–16, 2013.

[10] M.T. Lawder et al. "Battery Energy Storage System (BESS) and Battery Management System (BMS) for Grid-Scale Applications," *Proceedings of the IEEE*, vol. 102, no. 6, pp. 1014–1030, 2014.

[11] H.M.O. Canilang, A.C. Caliwag and W. Lim . "Design, Implementation, and Deployment of Modular Battery Management System for IIoT- Based Applications," *IEEE Access*, vol. 10, pp. 109008–109028, 2022.

[12] C.R. Sarin and G. Mani . "An Intelligent BMS With Probabilistic MOGSO Based CDMAS Integrating Edge Controller Analytics," *IEEE Access*, vol. 10, pp. 115802–115814, 2022.

[13] Matej Alandžak, Tomislav Plavsic, Dubravko Franković. Provision of Virtual Inertia Support Using Battery Energy Storage System, Journal of Energy – Energija, Vol. 70, No. 4, pp. 13–19, 2021

[14] "Smart Grid Laboratory (SGLab)," Faculty of Electrical Engineering and Computing, Department of Energy and Power Systems, University of Zagreb, [Online]. Available: https://sglab.fer.hr/. [Accessed: 24. 06. 2022].

[15] "Varta Pulse Datasheet," VARTA Storage GmbH, [Online]. Avail- able: https://solar-distribution.baywa-re.de/out/media/8-Pulse VARTA pulse datasheet en V08.pdf. [Accessed: 27. 05. 2022]"

[16] "Instruction Manual Varta Pulse,", VARTA Storage GmbH, [On- line]. Available: https://seasolargroup.com/wp-content/uploads/2018/08/ Instruction Manual VARTA pulse UK.pdf. Accessed: [27. 05. 2022].

[17] "SIMATIC ET 200SP – the compact IO system for the control cabinet," Siemens AG, [Online]. Available: https://new.siemens.com/global/ en/products/automation/systems/industrial/io-systems/et-200sp.html. Accessed: [20. 05. 2022].

[18] "SIMATIC ET 200SP Product Information," Siemens AG, [On- line]. Available: https://mall.industry.siemens.com/mall/en/WW/Catalog/ Products/10144488?tree=CatalogTree. Accessed: [20. 05. 2022].

[19] "CPU 1512SP-1 PN Product Information," Siemens AG, [Online]. Available: https://mall.industry.siemens.com/mall/en/WW/Catalog/Products/10239949?activeTab=productinformation&regionUrl=WW. Accessed: [22. 05. 2022].

[20] "SIMATIC HMI TP1200 Comfort Datasheet," Siemens AG, [Online]. Available: https://mall.industry.siemens.com/mall/en/it/Catalog/Product/6AV2124-0MC01-0AX0. Accessed: [09. 01. 2023].

[21] "Introduction to Modbus using LabVIEW," National Instruments, [Online]. Available: https://www.ni.com/en-rs/innovations/white-papers/12/ introduction-to-modbus-using-labview.html. Accessed: [21. 03. 2022].

[22] "Modbus/TCP with instructions 'MB CLIENT' and 'MB SERVER'," Siemens AG, [Online]. Available: https://support.industry.siemens.com/ cs/attachments/102020340/net modbus tcp s7-1500 s7-1200 en.pdf. Accessed: [21. 03. 2022]."

Journal of Energy

VOLUME 71 Number 2 | 2022

journal homepage: http://journalofenergy.com/

Mechanical and 1st Chemical Cleaning of NEK Steam Generators

Robert Kelavić, Marko Turalija

Summary — **Sludge removal is performed on two steam generators (SG's) at the Krško Nuclear Power Plant (NEK) during every outage. SG's are a meeting point of five major plant systems: Reactor Coolant System (RC) on the primary side and four systems on the secondary side – Auxiliary Feedwater System (AF), Blowdown System (BD), Main Feedwater System (FW), and Main Steam System (MS). Sludge removal activities take place on the secondary side of the SG's on the top of the tube sheet. It always consists of classical Sludge Lancing (SL) which is done by spraying water at different angles (30°, 90°, 150°) between the tube gaps in the steam generator tube bundle with a pressure of around 220 bars. Another method is Inner Bundle Lancing (IBL) which means spraying water directly inside the tube bundle with a traveling lance tape with a spraying nozzle at the end. Water is sprayed at an angle or directly on the top of the tube sheet with a robot-guided manipulator which is placed inside a steam generator. The manipulator and therefore the spraying action is controlled by an operator and at times it is fully autonomous to provide the highest protection measures possible. Another method of sludge removal which was for the first time utilized in 2019 at the Krško site was Chemical Cleaning (CC) of both SG's. During this process, a chemical was injected into the SG's through the BD system and periodically pumped between the two SG's to create a dynamic flow and maximize the cleaning effect. To achieve the best results, a constant temperature of the chemicals had to be maintained at all times. Upon completion of chemical cleaning, a rinsing phase was followed to remove any post-treatment chemicals. After all sludge removal activities, a televisual inspection (TVI) of the top of the tube sheet was performed to access the hard sludge area and to search for potential foreign objects in the SG's. If for instance an object of importance during TV inspection is found, an attempt to retrieve it would usually take place. Other methods of sludge removal such as upper bundle flushing or ultrasonic cleaning have not been implemented in NEK thus far. Since the power plant uprate in May 2000, NEK conducted SL on both SG's every outage also starting with IBL in 2013 and 2015, and the same method was used in the 2018 outage. During the outage in 2019, all three methods (SL, IBL, and CC) have been utilized with the main purpose to extend the full load operation of the plant, preventing and/or stopping denting processes in the SG's from occurring, reducing and stopping the build-up of hard sludge area to increase/sustain efficiency and remove foreign objects found in the SG's.SG's U-tubes are a barrier between the primary side coolant and the secondary side of NEK and the environment. Therefore, it is crucial to keep the highest level of integrity of the U-tubes because any leak could potentially mean a release of radioactive material into the atmosphere. This paper describes the purpose and workflow of sludge removal activities in the outage of 2019 in NEK.**

Keywords — **Steam Generators (SG's), Sludge Lancing (SL), Inner Bundle Lancing (IBL), Chemical Cleaning (CC), televisual inspection (TVI), Foreign Object Search and Retrieval (FOSAR), Krško Nuclear Power Plant (NEK)**

(Corresponding author: Robert Kelavić)
Robert Kelavić and Marko Turalija are with the Nuclear Power Plant Krško, Zagreb, Croatia (e-mail: robert.kelavic@nek.si, marko.turalija@nek.si)

I. Introduction

NEK's steam generators are safety related components that are required to operate during normal, abnormal, and emergency conditions. During normal power operation, steam from steam generators is supplied to the turbine. During shutdown conditions, they are vital components in the decay heat removal process. Additionally, steam generators act as a third barrier for preventing radioactive releases into the environment. Due to this the cleanliness and operability of steam generators are vital for safe operation.

The driving factor to perform the Chemical Cleaning process at NEK was the discovery of the denting indications in 2018, which have also been confirmed later by re-evaluation of old Eddy Current Testing (ECT) data from 2006 and 2012. Denting is tube deformation due to material ingress into the space between the tube and tube sheet (for details see Chapter 2).

For SG #1 there was a significant increase in the hard sludge area between 2010 and 2016 which has been observed in the hot leg and is being constant until the last visual inspection in 2018- before CC. From the past data re-evaluation, there were 33 denting indications discovered in the hot leg, which were detected in 2006 and 2012. They are all located not only in the hard sludge area but also in its periphery. Since 2012 no new denting indications have been detected in the hot leg. The hard sludge area in the cold leg detected in 2012 and 2018 but were not detected in 2016, which is classified as an inconsistency. The 5 denting indications first time detected in the cold leg in 2018 are located in the hard sludge area and the low-flow zone. The low-flow zone was determined by Computational Fluid Dynamics (CFD) calculations.

For SG #2 there was a significant increase of hard sludge area between 2010 and 2016 in the hot leg, which has been constant until the last visual inspection in 2018 before Chemical Cleaning (CC) (similar to SG #1). In 2012 detected denting indications are located mainly outside of the hard sludge area seen in 2010. The newest detected indications in 2018 are located mainly in the periphery of

the hard sludge deposits. On the cold leg side of SG #2, no denting indications occurred.

In total at the end of the outage in 2018, NEK had confirmed 121 denting indications on both SG's collectively.

Mechanical sludge removal activities take place on the secondary side of the SG's on the top of the tube sheet. It consists of regular Sludge Lancing (SL) which is done by spraying water at different angles (30°, 90°, 150°) between the tube gaps in the steam generator tube bundle with a pressure of around 220 bars. Another method is Inner Bundle Lancing (IBL) which means spraying water directly inside the tube bundle directly on the top of the tube sheet with a robot-guided lance which is placed inside a steam generator. The robot is controlled by an operator and at times fully autonomous to provide the highest protection measures possible. After these activities, a televisual inspection (TVI) of the top of the tube sheet is performed to access the hard sludge area and to search for potential foreign objects in the SG's. If an object is found, an attempt to retrieve it would usually take place.

This paper describes the chemical cleaning process that took place during the outage in 2019 and the mechanical sludge removal process in NEK in the same period. Descriptions from setting up the equipment, differences between Sludge Lancing and Inner Bundle Lancing, additionally the purpose of TV inspection and FOSAR attempts will be included. The paper will offer an insight into the results of this year's outage as well.

II. Degradation Mechanism Denting

Denting is the mechanical deformation of the Steam generator tubes due to the external pressure forces acting on the outer diameter. When rapid growth of the material trapped in the crevices of tube-to-tube sheet occurs it causes a reduction in the tube diameter. Historically this degradation mechanism was mostly reported in crevices between tube-to-tube support plates, but recently the mechanism is seen as in NEK case in the tube-to-tube sheet locations despite the better tube material (690) than historically more susceptible alloy 600 and alloy 800.

There are two contributing factors for denting mechanism to occur. The first precondition is the existence of metallic iron in the crevice which can be present due to carbon steel tube sheet or due to the ingress of ferritic particles originating in the secondary water-steam cycle of the NPP.

A second contributing factor is the presence of oxygen in the area of said ferritic material. That leads to a rapid expansion of the volume of the impurities and thus affecting the outer/inner tube diameter. If the crevice is exposed to additional corrosive impurities the reaction is only accelerated by interacting with basic tube sheet material – often carbon steel. Since Top of Tube Sheet (TTS) hard sludge area is present in Krško SG's it blocks the free expansion of interacted materials thus causing them to deform SG's tubes.

The formation of the initial crevice in a tube-to-tube sheet is a consequence of the manufacturing process. Since it was not advisable to expand the tubes till the very top of the tube sheet due to the possibility of overexpansion and causing an initial crack, the hydraulic expansion was suspended 1~2 mm below TTS and therefore creating a small crevice in the described area.

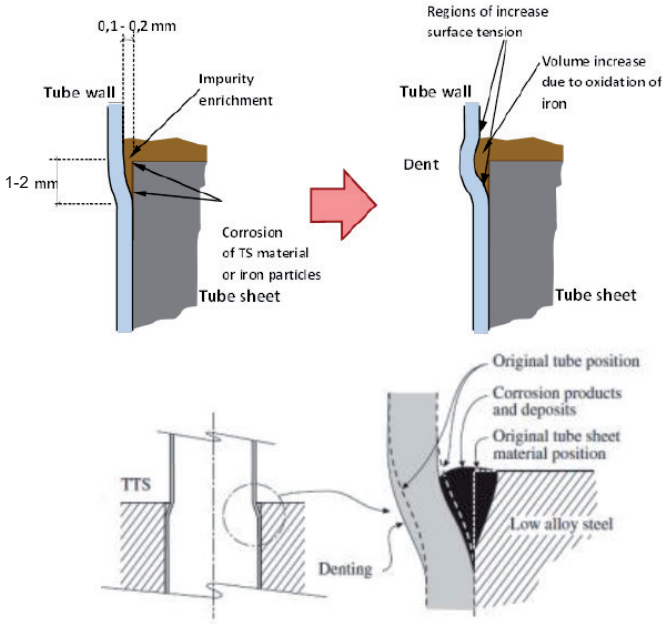

Fig. 1: Origination of dents on TTS

Regulation dictates that all tubes of SG must be checked with ECT every 5 years. ECT probes must fulfill something known as Fill Factor, which dictates that the probe diameter must be at least 80 % of the SG tube inner diameter. If the tube is inaccessible or its diameter is reduced due to excessive denting which causes that the fill factor criteria can't be met, the tube must be plugged preventatively. In the worst-case scenario denting can cause Outer Diameter Stress Corrosion Cracking (ODSCC).

2.1 Mitigation of denting

Denting can be mitigated with two main preventive actions and one corrective.

Firstly, the goal should be to limit particulate releases in the secondary water-steam cycle. This can be achieved by adhering to strict pH control or use of erosive/corrosive resistant materials, operating in steady state conditions, or injection of Film Forming Amines.

Secondly, the goal should be to limit oxygen levels in the secondary water-steam cycle. This can be achieved with strict control of Feed Water (FW) during On-Line (OL) operation, strict control of Auxiliary Feedwater (AF) during startup and shutdown, conservation of the secondary side of SGs with hydrazine, wet layup, and Film Forming Amines (FFA) during an outage.

Thirdly, the curative action is to remove the particulates accumulated on TTS. This can be achieved with the use of Blow Down (BD) system, Sludge Lancing (SL), Inner Bundle Lancing (IBL), chemical cleaning, Upper Bundle Flushing techniques, or installation of CY magnets. Newer options for sludge removal are the use of Poly Acrylic Acid (PAA) dispersants.

III. Chemical Cleaning – Flow of Events from the Decision to Execution

After the denting discovery in outage 2018, the technical debate was convened in NEK, where a mitigating strategy was presented and the decision for chemical cleaning in outage 2019 was formalized. Since NEK had no previous experience a benchmark of two NPPs that have performed where utilities used two different CC vendors. The first NPP was ASCO in Spain and the second was Belleville, France. This led to the realization of important

Robert Kelavić, Marko Turalija, Mechanical and 1st Chemical Cleaning of NEK Steam Generators, Journal of Energy, vol. 71 Number 2 (2022), 10–17
https://doi.org/10.37798/2022712413

factors the chemical cleaning process had to assure. The scale of equipment used for chemical cleaning had to be small enough to fit in the planned NEK area. Additionally, the process had to be efficient to clean the desired hard sludge area on TTS. Also, the process had to "fit" into the planned time schedule of the 2019 outage plan.

The bidding process was finished in March of 2019 and the selected vendor was Framatome GmbH for CC and mechanical cleaning operation. NEK had performed the QA audit the following month and received the "NEK Replacement Steam Generator Assessment Study" the month after. The study analysed a wide range of secondary chemistry data, the result of which was a selected process for chemical cleaning called DART LT - Deposit Accumulation Reduction Treatment at Low Temperatures with EDTA (95–100 °C). In June Adaptation study document followed which in detail defined the chemical cleaning procedure. Several performance tests were running simultaneously as well as presentations to the Slovenian regulatory body, Krško Safety Comitee (KSC), and internal organization. Additional walkdowns were performed and an equipment laydown area was prepared to facilitate the planned equipment.

IV. Setup of equipment

The arrival of equipment and its security check took place on 26/9/2019. The equipment was set up in the following days, which included the two separate units for SL and IBL processes both equipped with separate filtration systems and a Chemical injection container, two equipment containers, 2 additional quick shop containers, one large Waste sump trailer, and one insulated trailer for DD water, 4 TRAMETHYN – EDTA IBC double wall storage tanks, Severe Accident Mitigation Equipment (SAME) air compressor, and some additional spare equipment container.

The equipment was placed on the west side of the TB next to CY storage tanks.

Fig. 2: Equipment setup outside Reactor Building

Cable and hose routing was set up through Intermediate Building 100 (IB 100) elevation and consequently to Reactor Building (RB)100 and RB107 upon emergency hatch opening. Additionally, the heaters used for chemical cleaning and the distribution control were set up in IB100 as well to be as close as possible to SG's and to maximize the efficiency of the process.

After the arrival of personnel, a detailed pre-job briefing and basic general employee training were conducted. For of chemical/mechanical cleaning containment integrity is not required, so as soon that's the case, the equipment inside the RB and outside of it is connected and water was recirculated through both systems to ensure a leak-tight connection. During the first recirculation, a water sample is taken to prove the cleanliness of the cleaning equipment before the introduction of that water inside the NEK's SG's.

V. Operation

5.1 Chemical cleaning

The proposed sequence of sludge removal process was:

- SL1 on SG #2, Drying, TVI1 on SG #2 + FOSAR;
- CC on SG #1 and SG #2;
- Rinsing of SG #1 and SG #2 after CC;
- SL1 on SG #1, Drying, TVI1 on SG #1 + FOSAR, IBL on SG #1, SL2 on SG #1, Drying, TVI2 on SG #1 and FOSAR2;
- IBL on SG #2, SL2 on SG #2, Drying, TVI2 on SG #2 and FOSAR2.

The reason for the difference in the cleaning sequence was that SG #2 had reported foreign object (FO) in the non-desirable area during the 2018 outage and it was desirable to retrieve it first. Another reason was to maximize the efficiency of the chemical cleaning process, the RCS had to be drained as to prevent the heat reduction of the chemicals if it were to "escape" to the primary system through filled SG tubes.

5.2 Sludge Lancing (SL)

An SL robot is positioned and operated in the NO-Tube lane to remove the loosened sludge accumulated inside the hot leg (HL) and cold leg (CL) out of the tube bundle. The water is directed to the SG through high-pressure (HP) pumps (200 bar and 250 bar). Then the mixture of water plus sludge is removed from the SG by diaphragm pumps and trapped by high-performance filtering elements. The water is then conducted to a storage tank, to be re-injected into the steam generator by high pressure and peripheral jets pumps (see Figure 1). A bypass loop cools the water from the storage tank and purifies it so the SL cleaning process uses as neutral water as possible inside the SG's.

Because of the triangular pitch of the Krško SG's, the SL robot can be used in a 90° direction and 30°/150° from the NO-Tube lane. With the orientation of the jet stream in the direction of 30°, 90°, and 150°, it is possible to reach both a higher number of passes of the HP jets and various areas of the tube bundle compared to cleaning only at 90°. In this manner, the "shadow areas" which are behind the U-tubes from the perpendicular direction of the NO-Tube lane are also reached and cleaned.

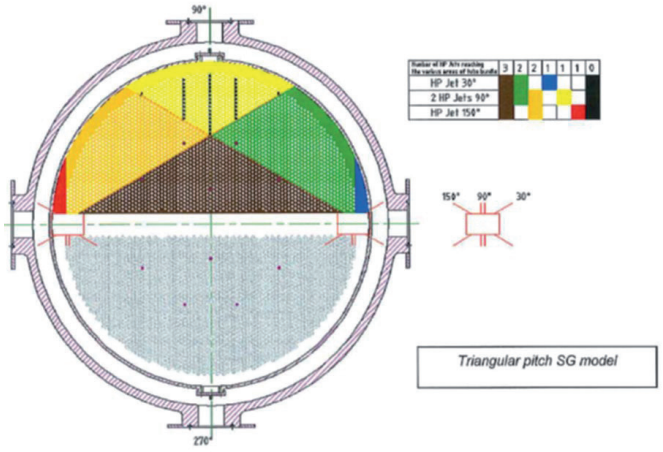

Fig. 3: Direction of High Pressure (HP) jets inside SG during the sludge lancing phase

Robert Kelavić, Marko Turalija, Mechanical and 1st Chemical Cleaning of NEK Steam Generators, Journal of Energy, vol. 71 Number 2 (2022), 10–17
https://doi.org/10.37798/2022712413

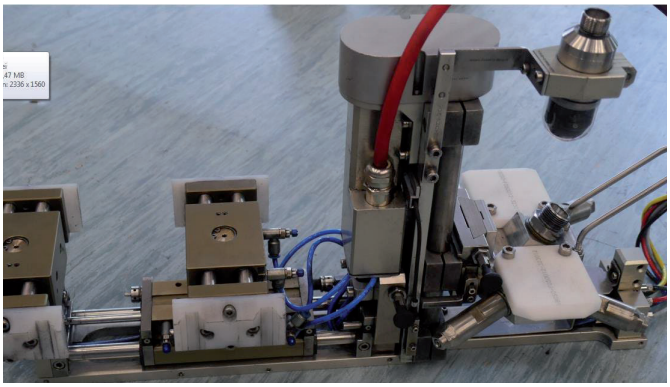

Fig. 4: SL manipulator

5.3 Inner Bundle Lancing (IBL)

A manipulator installed in the NO-Tube lane is equipped with an HP lance which can enter between tubes. Its goal is to break hard sludge deposits inside the tube bundle in the very low-velocity water area. The lance can be guided at a 90° angle and can reach the farthest area of SG tube rows. IBL lance travels between the tube bundle at different heights depending on the hard sludge situation. The spray head is spraying at a 60 ° angle which is constantly adjusted by the software program.

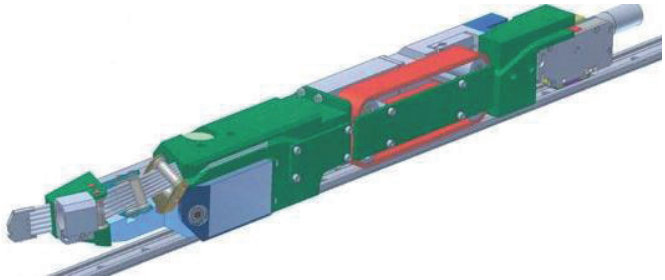

Figure 5: IBL manipulator

5.4 Drying

After SL, the SG must be prepared for TV inspection. Due to high humidity inside the SG after SL/IBL phase, the camera lens could get foggy and the image becomes blurry, therefore the drying equipment is introduced. The drying equipment consists of two intake units with HEPA filters, a double fan unit with a heater, and connection hoses. The discharge hoses are connected to the SG's inspection holes in the direction perpendicular to the NO-Tube lane. At least one secondary manway must be opened to effectively dry the SG before TV inspection. This process lasts about 10 hours.

5.5 TV inspection and FOSAR

Remote visual inspection is performed to inspect the inner tubes on the tube sheet, after the Sludge Lancing, to check the cleanliness, locate eventual foreign objects and check the result of the Sludge Lancing. A manipulator works the same as the IBL one, but instead of a high-pressure tape, the system uses a camera tape for inspection. Additionally, as a backup the vendor uses a crawler moving in the NO-Tube lane. The lance goes into each inter column at 90°, from the NO-Tube lane to the peripheral lane. The gap between each U-tube is approximately 3.6 mm when the tubes are new and no sludge has been accumulated. A small layer of sludge on the tube can block a camera path regardless of the fact, that the lens is only 2.7 mm thick. Another obstacle inside the SG is the space between a Tie-Rod and a U-tube.

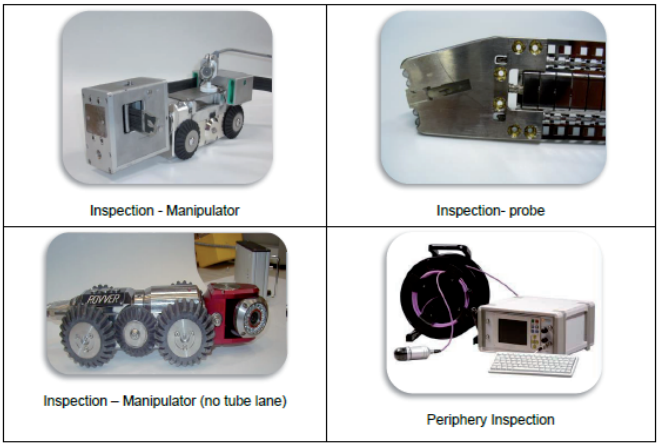

Fig. 6: TVI inspection tools

If a foreign object is found inside the SG, its location is carefully noted, the object is categorized, its length, weight and material is approximated. The categorization is carried out using the EPRI Technical Report 1020989 Steam Generator Management Program: Foreign Object Prioritization Strategy for Triangular Pitch Steam Generators. Based on the shape, size, and position of the object, its general location inside the SG, and some other factors, a decision will be made if a retrieval attempt is performed. TV crawler in that case acts as a guide for the operator who manually inserts the tool and tries to grab the object stuck inside the SG. The success rate of these attempts varies and depends mostly on the skill of the operator of the FOSAR tool and experience. If an object is retrieved, a detailed analysis is conducted to determine its origin and structure. If the attempt fails, the location is reported and ECT inspection of the contact and surrounding tubes is performed at the shortest possible interval. Some objects are monitored during the entire time of operations in the SG's.

VI. Results

6.1 Introduction

The results of mechanical and chemical cleaning of the Krško NPP steam generators in the outage of 2019 are satisfactory, particularly in terms of the amount of removed sediment: 223 kg out of an estimated 290 kg. The estimation included total sludge inventory in the tube sheet area up to a height of approximately 1m. However, we can be less satisfied with the fact that we have not been able to clean both top-of-tube sheets (TTS). After the finished activity and "Lessons learned" we can now summarize the influencing factors, good and bad experiences, and give an evaluation of performance.

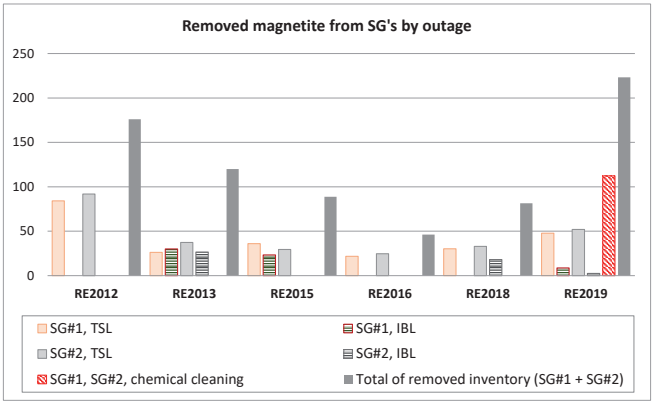

Fig. 7: Balance sheet of removed magnetite from SG's since 2012

Robert Kelavić, Marko Turalija, Mechanical and 1st Chemical Cleaning of NEK Steam Generators, Journal of Energy, vol. 71 Number 2 (2022), 10–17
https://doi.org/10.37798/2022712413

6.2 The short duration of the chemical phase (minus grade)

In October 2018, the length of the chemical cleaning activity was set based on the maximum length of the planned outage which was 28 days. At that time, the planned duration of the chemical phase was 80 hours, although the contractor's recommendation was from 100 to 110 hours. In addition, the "Performance Test" was performed at a time of t ≈ 100 hours. Due to other interconnected activities such as SL, IBL, VT, and FOSAR, no additional time was available in the overall Outage Plan.

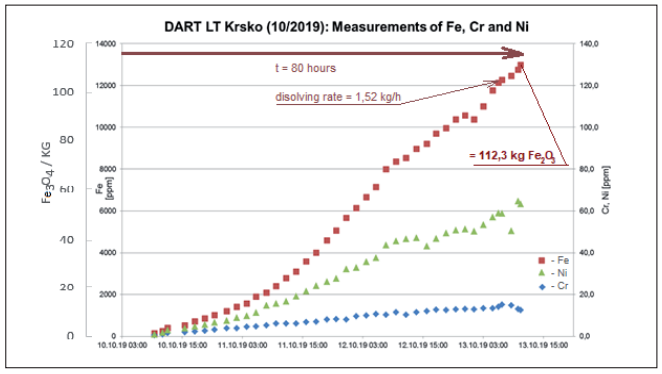

Fig. 8: Concentration rate of Fe, Cr, and Ni in EDTA solution during NEK application

At the moment when the dissolving rate of Fe was 1.52 kg/h, we discussed the possibility of process extension. The contractor proposed to extend it to 94 hours, which would provide 6 hours of "Safety margin" based on the 100-hour "Performance Test" qualification. We organized a meeting to extend the activity on the critical path, but during the meeting trend slowed down and the additional extension time was not agreed upon. Assuming that the chemical cleaning phase was prolonged, likely another 25 kg of Fe or more would be dissolved (1.36 x 25 = 34 kg Fe_3O_4). This would further improve the overall balance and reduce the hard deposits area. It should also be noted here that the amount of dissolved Ni and Cr was much lower in the chemical treatment than in the Qualification Performance Test, which means that there was no significant impact on the materials or systems.

Table 1

Removed sludge balance sheet

Removed sludge balance sheet (SG #1 & #2 in R´19 /out of 290 kg estimated)		
	SG #1 [kg]	**SG #2 [kg]**
1. SL		32,65 (before C.C.) *
Chemical cleaning ∑ (SG#1 + SG#2)	112,3	
1. SL	18,18 (after C.C.)	
IBL	8,598	2,536
2. SL	29,663	19,342
∑ (SL+IBL)	56,445	54,528
Mechanical cleaning ∑ (SG#1 + SG#2)	111,0	
∑ (CC + MC)	**223,3**	

* Since SL was performed on SG #2 before CC, it is believed that was the reason for an overall cleaner TTS on SG#2

6.3 Chemical composition of soft and hard sludge and influence on the chem. dissolution rate (minus grade)

2019 outage dissolutions of Fe or. Fe_3O_4 in EDTA solution was significantly slower and smaller in the site-implementation process than in the Performance Qualification Test under laboratory conditions at contractors' facilities, where previously removed (soft) sediment from the Krško NPP was used.

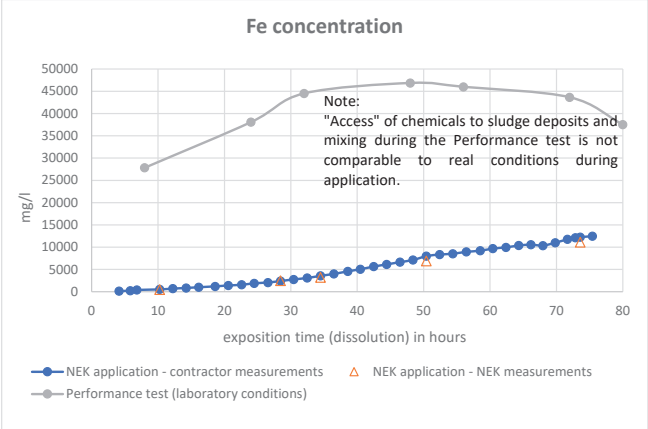

Fig. 9: The dynamics of real-life dissolution in the Krško NPP compared to the Performance Qualification test.

Some influential factors that have reduced solubility and slowed down the process can be identified:

- The hard sediment in the steam generator is compact, a kind of "concreted magnetite" that has been formed layer after layer since the replacement of SG's in 2000. Magnetite used in the "Performance test" was in the form of soft sludge like wet powder compared to hard sediment in the steam generator that had to be dissolved layer after layer again. The process was therefore slower and less efficient than in the laboratory.
- Mixing the medium in a laboratory autoclave was much more efficient than with the actual process in steam generators, where the tube bundle represents a large hydrodynamic flow resistance. Kinetics of a chem. reaction in the steam generators was, therefore, smaller and the process slower.
- The chemical composition of soft sludge is not the same as that of hard sediment. The presence of silicon (Si) and aluminium (Al) is known to have a negative effect on the dissolving of magnetite because it promotes the formation of highly resistible deposits. The last exact chemical composition of sediments is from the outage of 2012. The Si content increased from 2004 (the first analysis of sludge morphology) to 2012. Al in sediments (2004, 2006, 2009, and 2012) has not been reported.
- The laboratory can efficiently control the temperature during the whole process whereas the real-life application experiences some variations during this time.

6.4 Comparison of SG #1 and SG #2 cleaning sequence (plus SG#2 assessment)

Due to the outage plan and the fact that SG #2 was available earlier, the cleaning sequence started before SG #1. The proposal to start with SL (Sludge Lancing) was accepted, so the sequence of activities on both was a little different, which in the end contributed to a more efficient sludge removal on SG #2. The sequence of activities was:

Robert Kelavić, Marko Turalija, Mechanical and 1st Chemical Cleaning of NEK Steam Generators, Journal of Energy, vol. 71 Number 2 (2022), 10–17
https://doi.org/10.37798/2022712413

Table II

Comparison of SL1 between SG #1 and SG#2 before and after CC

Comparison of SL1 between SG#1 and SG#2 before and after CC		
	SG #1 (kg)	**SG #2 (kg)**
1. SL (Sludge Lancing)	18,184 (after C.C.)	32,650 (before C.C.)

From the large amount of soft sediment removed on SG #2, it was be concluded that on SG #1 a chemical dissolution of soft sludge took place which could have been removed by SL if the sequence of sludge removal was the same as on SG #2. Based on chemical principles and kinetics, the chemical reaction of dissolving the soft granulate* is faster, rather than the hard layers of magnetite, which at that time were mostly covered with soft sludge. Access to hard sludge to EDTA was severely restricted and this is the reason that the chemical dissolution of hard sediment at SG #1 was not as effective as at SG #2. Basically, at SG #1, we believe we used a chemical process to remove a lot of soft sludge that would be easier to remove with SL. Therefore, the final mass of sludge was smaller. (Soft granulate*: a mixture of dust and small moving particles of soft sludge of different sizes on the TTS).

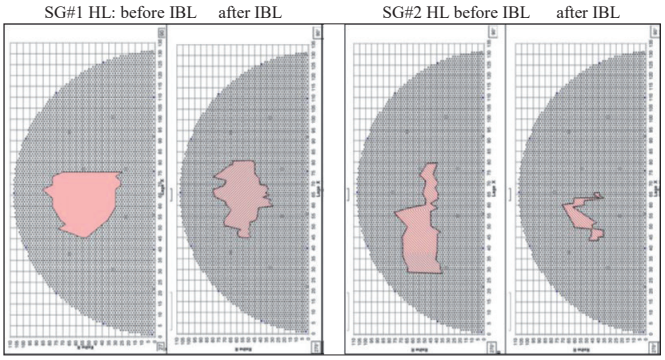

Fig. 10: Hard sludge deposits on Hot Legs of SG#1 and SG#2 before and after IBL

The surface area of hard sludge at the top of the tube sheet (TTS), which is a basic precondition for the formation and progression of the denting mechanism, decreased largely on SG #2 than it did on SG #1 after all removal activities. We expected similar sludge removal efficiency on both SG's but the distinction in the sequence of the mechanical and chemical cleaning process is probably the reason for the resulting differences.

6.5 Scraping / peeling off of brittle scales on SG tubes (plus grade)

Before the final VT (visual inspection) of the tube sheet, where foreign bodies were registered and the size of the area with hard sludge was determined, the plan was to dry the tube bundle with hot air as in previous outages. As a result of drying, peeling of a thin layer of hard scales on the tubes occurred. This is probably due to a combination of chemical cleaning and later hot air drying, which led to an uneven expansion of the scaling material and tubes of the steam generator (Figure 5). The result was a large amount of magnetite "scales" that were washed into the BD system and not taken into account in the final mass balance of removed sludge.

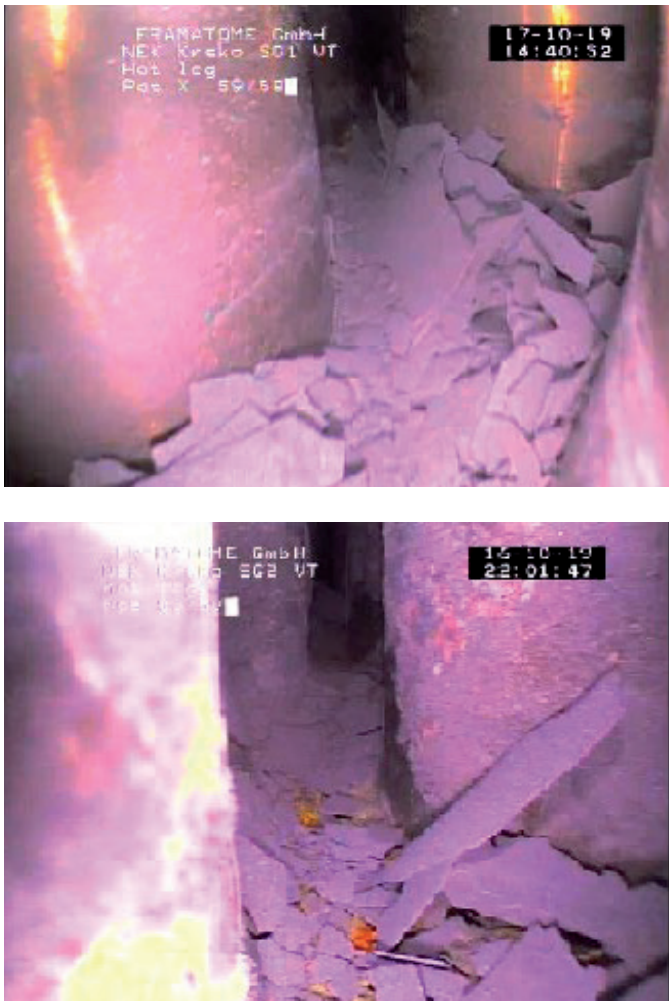

Fig. 11: Fallen scales of magnetite after SG drying phase

6.6 Appearance of a large number of foreign objects and their classification (plus grade)

Chemical cleaning was used to dissolve the hard sludge at the top of the tube sheet, which also revealed some foreign objects that were in deeper layers and had never been discovered before. The number of foreign objects is high, but most of them are thin wires that probably belonged to a wire brush.

Due to their weight and size the discovered foreign object are non-dangerous (classification: Type 1 / Category 3; Foreign Object Classification), but they leave a bad impression and they will have to be monitored in the future. If the process of accumulation of hard sludge continues, it will "disappear" over time. Their removal is not necessary and would often be technically impossible or at least very complicated and time-consuming.

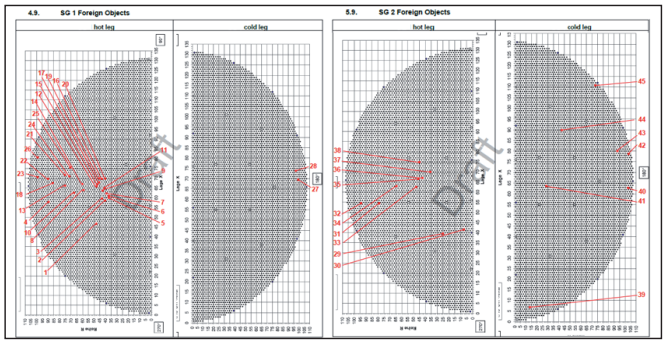

Fig. 12: Foreign object placement after outage 2019

Robert Kelavić, Marko Turalija, Mechanical and 1st Chemical Cleaning of NEK Steam Generators, Journal of Energy, vol. 71 Number 2 (2022), 10–17
https://doi.org/10.37798/2022712413

Limiting Object Categories[1,6]

Classification Type Number	Object Type Classification	Category 2 (Medium) Acceptable Object Dimensions (inch)[2]	Category 3 (Low) Acceptable Object Dimensions (inch)[2]
1	Wire[3]	2.5 long x 1/16 dia	1.75 long x 1/16 dia
2	Rod[4]	2.0 long x 1/8 dia	1.5 long x 1/8 dia
3	Rectangular Metal Objects	1/2 x 1/8 x 1/8	1/4 x 1/8 x 1/8
4	Machine Turning	1/2 x 1/8 x 1/8	1/4 x 1/8 x 1/8
5	Gasket[5]	1.75 long x 1/4 x 1/8	1.25 long x 1/4 x 1/8
6	Machine Remnant	1/2 x 1/8 x 1/8	1/4 x 1/8 x 1/8
7	Sludge Rock	1 x 1/4 x 1/4	3/4 x 1/4 x ¼ Or any size if soft or crumbles
8	Balls	1/2 Dia	3/8 Dia
9	Scale	-	Any size if soft or crumbles
10	Wire Bristle	3.0 inch Long 1/32 dia. - If small number found (no clumping found)	2.0 inch Long 1/32 dia. - If small number found (no clumping found)

[1]These object sizes are representative object dimensions based on two operational cycles or three years of plant operation. Actual part geometry, location, orientation and configuration may result in a more aggressive object and, therefore, would require a corresponding change to a higher priority.

[2]These sizes are based on finding the object in the annulus or on the tubesheet behind a tube. If the object is wedged between the tubes, it should be removed or a detailed engineering evaluation performed.

[3]Wires are semi-flexible objects.

[4]Rods are stiff objects.

[5]Assumes the object is lying flat against the tube.

[6]Sizes applicable for objects not located in red exclusion zone.

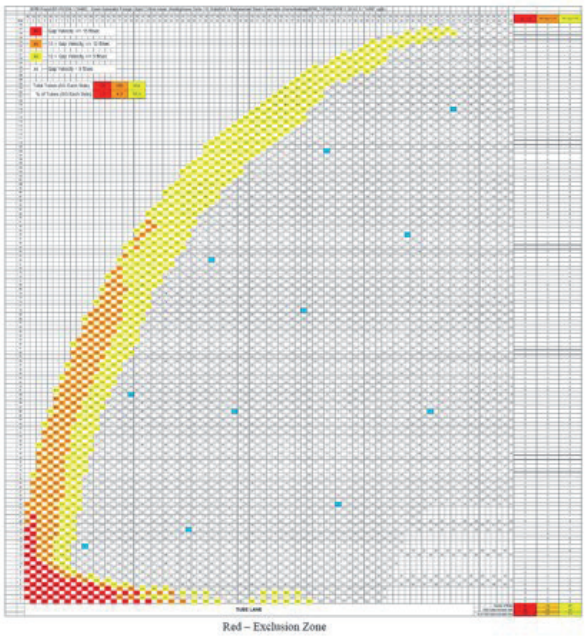

Fig. 13: Classification of foreign objects and the area of high hydrodynamic flow at the periphery of the SG tube bundle - EPRI summary SGMP TR 1020989

6.7 Chemical waste from completed chemical cleaning activity (plus grade)

At benchmarking at Asco NPP in Spain, information was received on the huge quantities of waste chemicals left in the yard after the activity was completed. This was mainly because the waste water showed traces of contamination and the recovery of the waste was not clearly defined in the contract. Therefore, we have included in the technical specification for procurement of the chemical cleaning activity that the contractor is responsible for the recovery and disposal of waste materials. The waste water was not contaminated in our case, so there were no problems in this area. The subcontractor took care of the rapid removal of chemical waste, which also avoided formal complications due to legal requirements for longer storage of this type of waste.

6.8 Removal of hard sludge in the area of DNTs from SG ECT R'18 and ECT reevaluation (2006, 2012, 2018), (SG #1 - minus grade, SG #2 - plus grade)

The primary goal of chemical cleaning was to clean the hard sludge area on the TTS under which the formation of the DNTs is taking place. After the 2018 outage, the ECT data from previous outages was reevaluated to determine when the denting mechanism appeared and with what dynamics it evolved. Statistical analysis of the data revealed that they were most extensively produced in the period 2006-2012, some of them even earlier. By evaluation of 2021 ECT data, it will be able to estimate the combined impact of 2 operational cycles, i.e. OL30 and cycle after chemical cleaning; OL31. Expectation is that we will not notice any progression on the dents around which the ″hard sludge″ has been removed.

Dent re-evaluation statistics also show large difference between the two steam generators. Therefore, it is best to comment on each one individually, but at the same time, it is necessary to evaluate the success of chemical cleaning in the critical area (hard sludge area) where the dents appear, because this can already predict the development or stagnation of this degradation mechanism.

6.8.1 SG #1 Hot Leg

ECT SG #1 in 2018 detected 33 dents on HL, which is essentially a small number based on the size of the ″hard sludge″ area. Interestingly, the 2006 denting mechanism was more developed at SG #1 (29) than at SG #2 (12). Nevertheless, the increment of a new dent at 6 cycles (2006-2012) was lower at SG#1. The right picture of the tube sheet shows the remaining ″hard sludge″ area after the 2019 chemical cleaning. The 2018 dent population has remained trapped in this area, which is not good. Optimistic about SG #1, however, is the fact that we only have 33 dents and that there were no new ones from 2012 to 2018. Since almost all dents have remained in the hard sludge area, we have to say that chemical cleaning on SG #1 HL did not fulfill expectations.

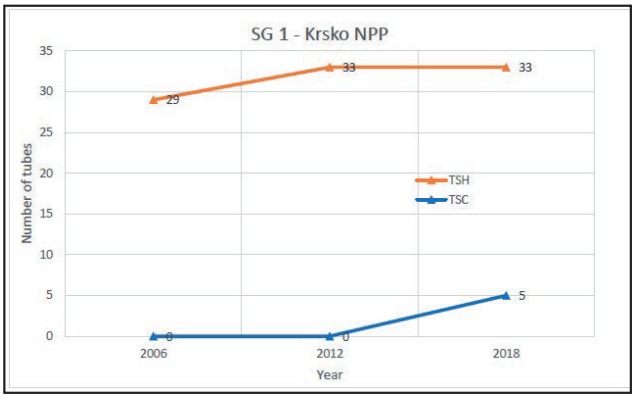

Fig. 14: Hard sludge area and DNT's after CC in SG #1 HL

Robert Kelavić, Marko Turalija, Mechanical and 1st Chemical Cleaning of NEK Steam Generators, Journal of Energy, vol. 71 Number 2 (2022), 10–17
https://doi.org/10.37798/2022712413

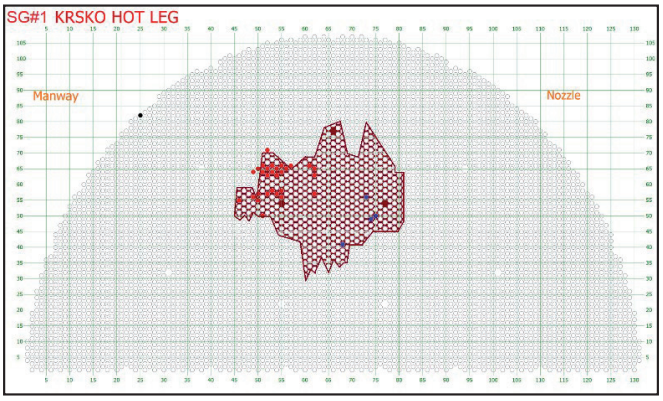

Fig. 15: Dent evolution on SG #1 HL (2002-2018)

6.8.2 SG #2 Hot Leg

ECT SG#2 in 2018 detected 83 dents on HL, 2.5 times higher than SG #1, although the hard sludge areas were comparable in size. The denting mechanism started slower than at SG #1, and its result is higher than at SG#1. Chemical cleaning was much more successful at SG #2 because it cleaned > 70% of the area in which the 2018 dents are located. This is far more important because the number of dents at SG #2 is much higher (83) as per SG #1 (33). It is here that we expect that the degradation mechanism will not develop further.

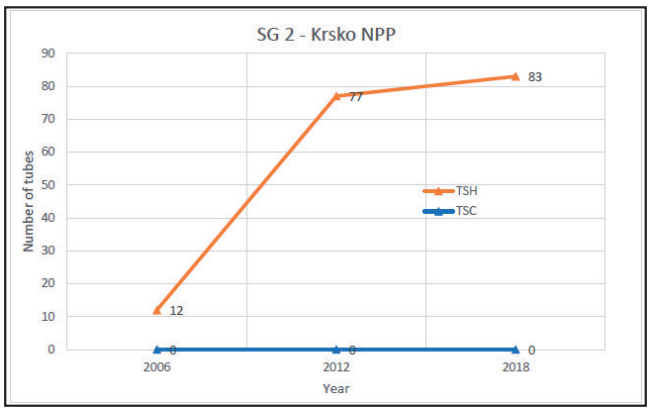

Fig.16: Hard sludge area and DNT's after CC in SG #2 HL

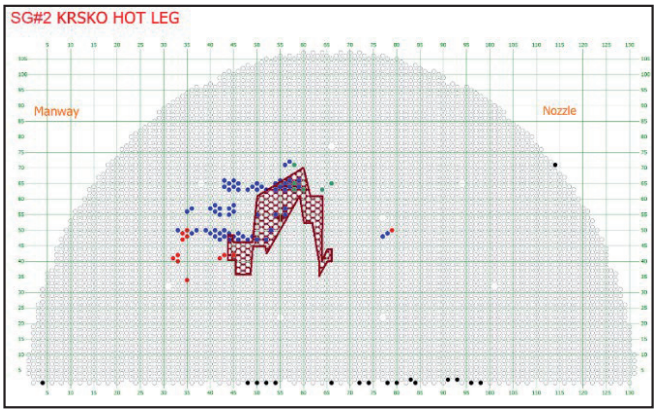

Fig. 17: Dent evolution on SG #2 HL (2002-2018)

With the projects implemented in the past cycle and the results, we have reached a much higher level of understanding of the degradation mechanism of denting, yet we still cannot explain why:

- more dents were generated on SG #2 (83) than on SG #1 (33),
- the number of the newly created dent was lower at SG #1 (4) than at SG #2 (65), in the period from 2006 to 2012
- the rate of newly formed dents decreased on both SG #1 (0 new) and SG #2 (5 new) in the period from 2012 to 2018

Evaluation of 2021 ECT data should provide some new answers. At that time, we will also be re-evaluating the dents from the second set of 50% ECT volumes (2021 – 2015 – 2009 – 2003). For the first time, we will also review the entire dent population - in the 100% scope in the same outage. This data will allow a final assessment of chemical cleaning, as well as an answer to whether the denting process has slowed down or even stopped. Should the trend continue or become even more intense, we can seriously think of repeating such a campaign.

At the moment, the results of statistics and predictions are not too pessimistic. In addition to that, some improvements are also planned that should make a positive contribution to water quality which supplies the FW system of steam generators. The final answer to the question of whether we need to do chemical cleaning in the area between the tube sheet and the first support plate again will be known after the following outages.

VII. Conclusion

In conclusion, the combined chemical cleaning and mechanical cleaning process met the expectations regarding the mass of sediment removed: 223 kg from an estimated 290 kg. The extracted amount equals to 77 % of the estimated, although the NEK goal was set around 80-90 %. The incomparable cleanliness of the hard sludge area especially on SG #2 was satisfactory which shall have a positive effect on the dent growth in the future. For SG #1 HL, the combination of the two cleaning methods fulfilled our expectation to some degree as we expect that due to the difference in the cleaning sequence the results were more visible on SG #2. Additionally, the CL sides of both steam generators were sufficiently cleaned as well. The most negative contributing factors that reduced Chemical Cleaning effectiveness were:

1. Short running time of the chemical cleaning phase (performed in t = 80 hours, which would require t ≥ 100 hours or more).
2. Activity sequence plan: likewise, on SG#1 the activity sequence should start with SL (Sludge Lancing), as it was with SG#2.

References

[1] NEK, "Efficiency Assessment of SG's – Sludge Lancing, Inner Bundle Lancing & Chemical Cleaning Activities During the Outage 2019 In NPP Krško", January 2020.

[2] "Replacement Steam Generator Assessment Study" Reference number: D02ARV01145105, rev. B, July 2019

[3] "Technical Description SL_VT_IBL_FOSAR" Reference number: F.031071-B-02, February 2019

[4] "DART LT NPP Krško 2019 - Final report" Reference number: D02-ARV-01-149-781, rev. A, December 2019

[5] "MC Technical Document for Final Report" Reference number: D02-ARV-01-149-200, rev. B, December 2019

[6] NEK CC project materials, July 2018 till December 2019

ENERGIJA